

INFLUENCE OF TRANSPARENCY OF PACKED BED ON MAIN PARAMETERS OF HIGH TEMPERATURE RADIATIVE BURNER

Dobrego K.V., Foutko S.I., Zhdanok S.A.

Heat and Mass Transfer Institute Belarussian Academy of Sciences,
Minsk 220278, P.Brovki 15

The optical properties of packed beds may differ significantly and influence on important characteristics of RB such as radiative efficiency of RB, maximum temperature of porous media, flame localization. We performed 1-D numerical simulation to investigate this influence as for opaque (Alumina spheres) and semi-transparent (Quartz glass spheres) packing. Results of comparison are discussed. The Differential Approximation (DA) was accepted for radiative heat transfer simulation. More detailed information about thermal and optical properties of ceramics one can find in [9,10].

To evaluate optical properties, average quantum path length was experimentally measured for a number of beds. To this end, samples of porous bedding layers were prepared of quartz grains of irregular shape, hollow and solid balls of opaque Al_2O_3 . Laboratory 0.62 μ He-Ne laser was used as radiation source. Photometer was used as detector. Bedding layer thickness was altered from 0.5 to 1 cm for solid balls and from 1 to 2.5 cm for hollows balls and quartz. Also experimental data by Chen, Churchill' 1963 were fitted for different temperatures of the source. Table 1 gives results of measurements and fitting.

Table 1. Quantum path length l_0 measured by transmittance of bedding and obtained from experiments by Chen, Churchill' 1963.

Bedding material	Particle size, mm	Porosity	Pore size L , mm	Measured l_0 mm
milled quartz	4	0.42	3.3	4.1
Hollow Al_2O_3 balls	3	0.38	2.5	3.8
Solid Al_2O_3 balls	2.8	0.38	2.3	2.3
-II-	5.6	0.38	4.7	53
Boro-silicat polished balls, $T_0=1366$ K	5	0.38	4.25	25
Boro-silicat polished balls, $T_0=922$ K	5	0.38	4.25	9

Problem statement and analysis

Consider one-dimensional axis-symmetric cylindrical system and isobar gas flux, neglect internal heat sources, except gas-phase chemical heat release, and assume that gas is optically transparent. Simulate chemical heat release by Arrhenius gross-reaction

Mathematical model of RB includes the equation of conservation of energy for gas and solid phase and balance of reacting reactant. Neglecting diffusion and heat conductivity in gas phase, compared to convective flows, obtain

$$c_p \rho \frac{\partial T}{\partial t} = \frac{1}{r} \frac{\partial}{\partial r} \left(\lambda r \frac{\partial T}{\partial r} \right) + \frac{\partial q}{\partial t} + \alpha (T_s - T),$$

(1)

$$c_s \rho_s \frac{\partial T_s}{\partial t} + c_s u_s \frac{\partial T_s}{\partial z} = -\alpha (T_s - T) + QW(y, T_s),$$

(2)

$$\rho_g \frac{\partial y}{\partial t} + \rho_g u_g \frac{\partial y}{\partial r} = -\rho_g W(y, T_g).$$

(3)

Here T is temperature, y is concentration of missing reactant, c is heat capacity, ρ - density, λ - heat conductivity, $\tilde{\nabla}q$ - radiant flux divergence, α - bulk heat transfer coefficient, u_g - gas filtration rate, Q - heat effect of reaction, $W(y, T)$ - chemical reaction rate. Subscript g is related to gas phase, solid phase parameters are without indices

System (1)-(3) is closed by the equation for chemical reaction rate, equation of gas state and equations for radiant energy density and radiant flux divergence in differential approximation

$$W(y, T_g) = yz \exp(-15640/T_g), \quad (4)$$

$$\rho_g T_g = \text{const}, \quad (5)$$

$$\nabla\left(\frac{\lambda}{\alpha r}\right) \nabla U - 4aU + 16a\sigma T_g^4 = 0, \quad (6)$$

$$\nabla q = 4a\sigma T_g^4 - c_0 a U, \quad (7)$$

where U is density of radiant energy, a , s are effective absorption and scattering factors, respectively, σ - Stephan-Boltzmann's constant and c_0 - velocity of light. Boundary conditions for equations (1)-(3) and (6) become

$$\left. \frac{\partial T}{\partial r} \right|_{r_0} = 0, \quad \left. \frac{\partial T}{\partial r} \right|_{r_2} = 0; \quad T_g|_{r_0} = T_0; \quad y|_{r_0} = 1; \quad \left. \frac{\partial U}{\partial r} \right|_{r_0} = 0, \quad |q|_{r_2} = \frac{c}{2} U|_{r_2}$$

Energy supply to RB is defined by the flow rate and heat content of combustible mixture $Q^+ = GQ$. Energy supplied is spent on radiation and heating of combustion products $Q^+ = Q_{rad} + (c\rho)_g G \Delta T_{2,g}$. If we define radiation efficiency of RB as relationship of energy emitted from the surface in the form of radiation to the energy supplied to the system, as a result of elementary transformations we come to

$$\eta = \frac{Q_{rad}}{Q^+} = 1 - \frac{\Delta T_{2,g}}{dT_{ad}}$$

(8)

Here $\Delta T_{2,g}$ is an excess of exhaust gas temperature over initial gas mixture temperature, dT_{ad} is adiabatic temperature of fuel combustion.

Major part of calculations was performed for methane-air mixtures with fuel concentrations corresponding to adiabatic combustion temperatures $dT_{ad} = 1200, 2000$ and 3000 K. Mass mixture flow rate per RB length unit was altered in a wide range, $G = 0.001-2.5$ kg/sec/m. Systems with internal radius $r_2 = 10$ cm and $r_2 = 25$ cm were considered. Heat conductivity of the carcass was assumed constant, the values of other parameters were selected as follows: $\lambda = 15$ W/m/K, $m = 0.4$, $d_0 = 5.6$ mm. Interphase heat transfer factor α was calculated according to Aerov, Todes, Narinskii' 1979. Computations were made for porous packed beds with high radiation transmittance (smooth quartz balls) and low transmittance - rough Al_2O_3 grains. Absorption and scattering factors for Al_2O_3 , where $\varepsilon = 0.6$. Absorption factor for quartz bedding was taken in accordance with Table 1 for the bedding of borosilicate glass, scattering being neglected.

Comparative characteristics were calculated for both bedding: radiation efficiency according to formula (1.31), maximal temperature of the carcass and stationary localization of combustion front (defined by coordinate of maximal gas phase temperature). In all computations combustion initiation was executed from inside RB, which allows to overcome indeterminacies of combustion front localization.

Fig.1 shows the results of RB efficiency (radiation efficiency) for transparent and opaque bedding, depending on fuel consumption, its heat content and dimensions internal radius) of RB carcass As follows from calculations, Efficiency of RB made of transparent bedding is higher than the efficiency of opaque one. The value of this excess $\Delta\eta$ slightly depends on RB radius and is somewhat higher for high-calorific fuels (higher dT_{ad}). Table 2 gives maximal values if this excess lot the conditions simulated. $\Delta\eta$ has a tendency to grow together with fuel consumption, has slightly pronounced maximum and somewhat decreases when approaching the largest possible flow rate Fig. 1 a), b). For higher ambient temperatures (typical for heat-treatment furnaces, etc), peal value is more pronounced, compared to total reduction of radiation efficiency.

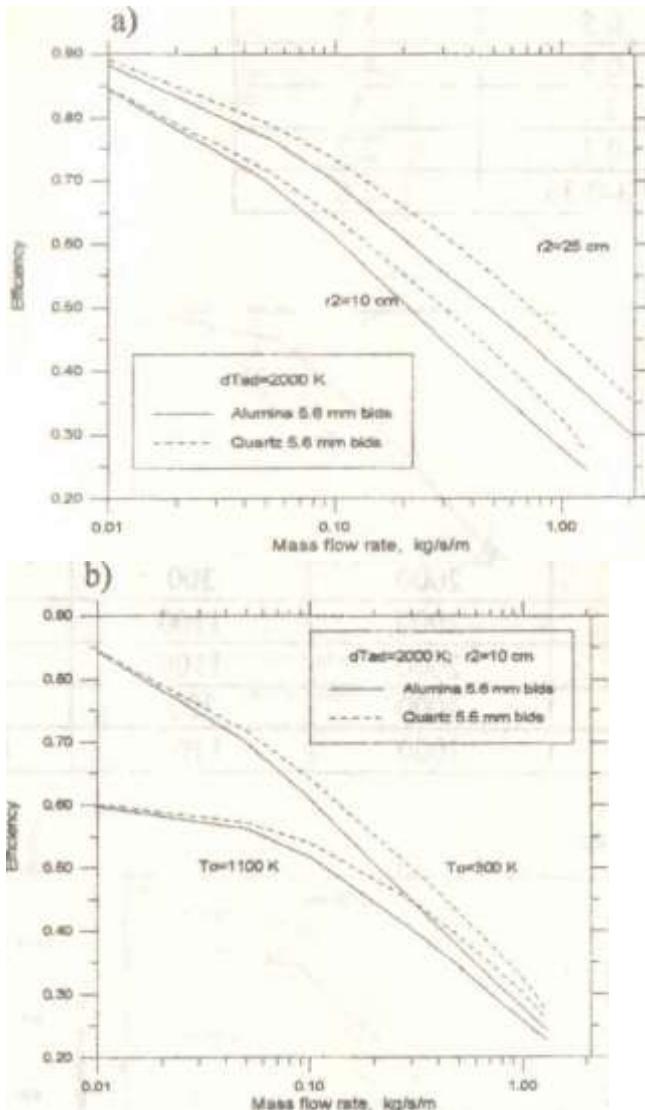


Fig. 1. Radiation efficiency of RB made of transparent and opaque beddings, depending on mass fuel flowrate. a) - for different external radii of RB. b) and c) - for different ambient temperatures T_0

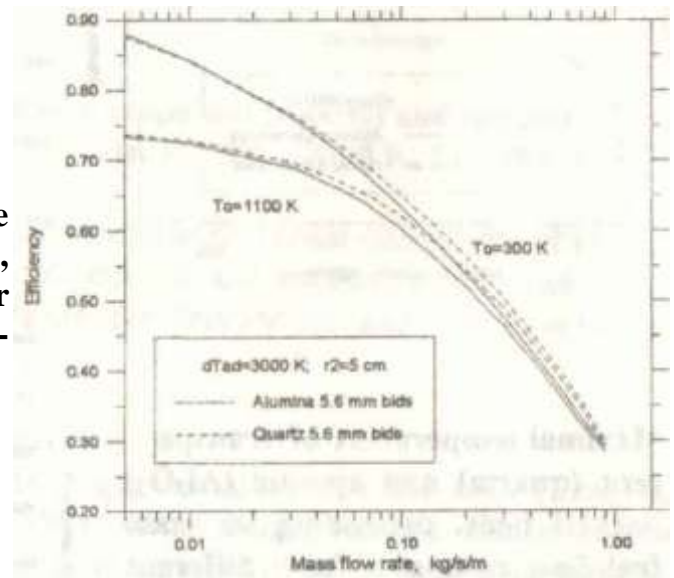


Fig.2. shows maximal carcass temperatures calculated for transparent and opaque bedding material. As follows from given results, largest temperature of transparent carcass is in average by 50 -150 K lower than that of opaque one (for the conditions under simulation). For more calorific fuels this excess is usually somewhat higher than that for poor mixtures. However, as seen from given plots, when increasing fuel consumption and calorific value and dimension of RB, maximal temperatures for transparent and opaque beds approach each other and inversion occurs for RB with larger radius ($r_2=25$ cm), i.e. largest transparent carcass temperature exceeds that of opaque carcass. Given unobvious situation is explained by the fact that opposing heat transport to incoming gas increases for transparent beds together with the growth of radiant heat losses from combustion front (compared to opaque ones), which results in higher level of heat recuperation, higher maximal temperature of gas phase and, as a result of interphase heat exchange, in higher carcass temperature and upstream shift of combustion localization. Since heat recuperation processes and losses from the

Table 2. Maximal difference of radiation efficiencies $\Delta\eta$ for RB made of transparent quartz and opaque Al_2O_3 beds

r_2 , cm	K	T_0 , K	G, kg/sec/m	$\Delta\eta$, %
10	1200	300	0.1	47
25	1200	300	0.1-0.2	5.1
10	1200	1100	0.15-0.2	2.5
25	1200	1100	0.45	2.5
10	2000	300	0.5	5.5
25	2000	300	0.5	5.9
10	2000	1100	0.5	4.8
25	2000	1100	15	5
5	3000	300	0.3	2.7
5	3000	1100	0.3-0.35	2.6

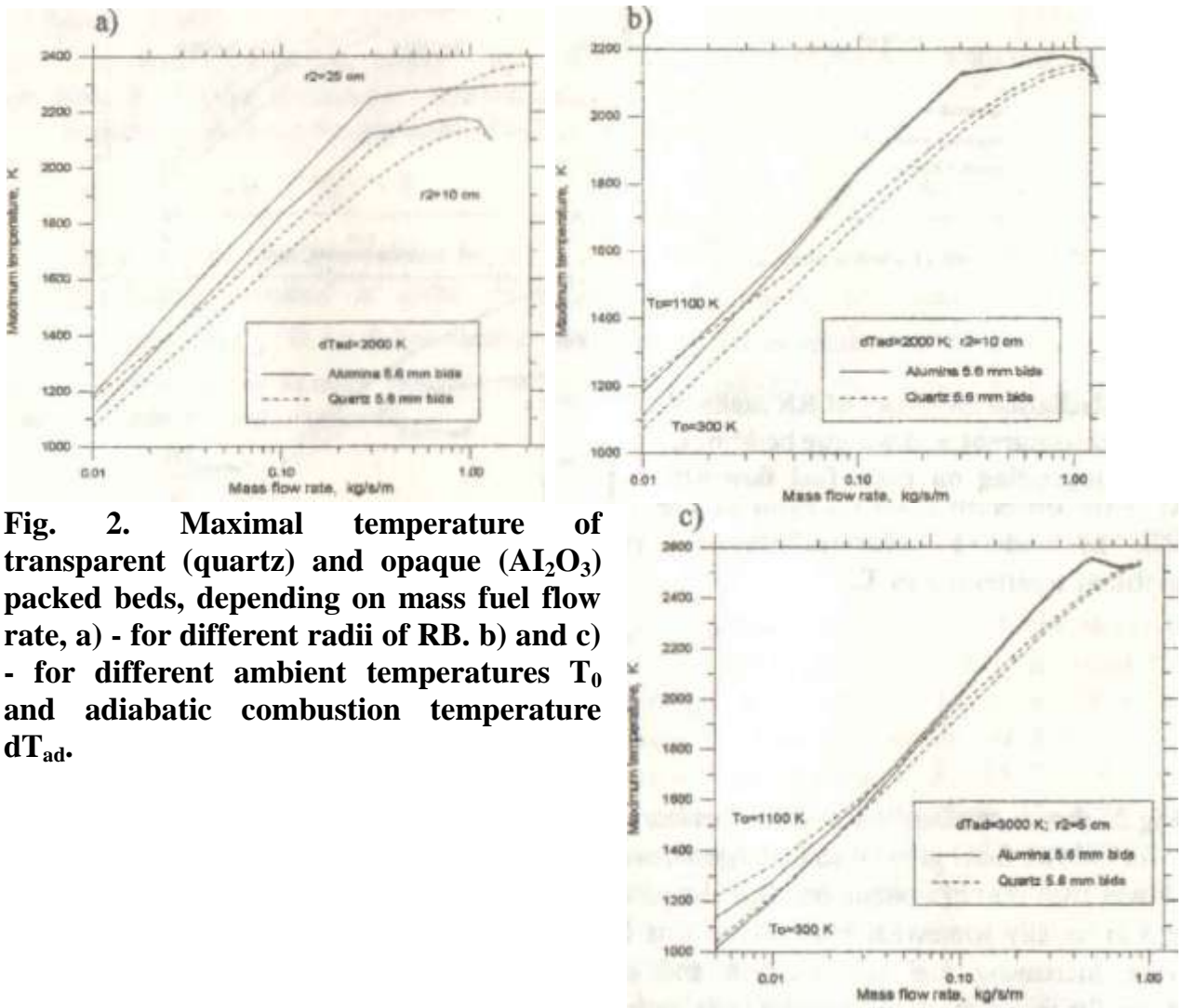


Fig. 2. Maximal temperature of transparent (quartz) and opaque (Al_2O_3) packed beds, depending on mass fuel flow rate, a) - for different radii of RB. b) and c) - for different ambient temperatures T_0 and adiabatic combustion temperature dT_{ad} .

front compete and exert opposite effect on carcass temperature, non-simple dependence of maximal carcass temperature on RB dimensions, mixture heat content and other parameters, observed in Fig.2, takes place. Thus, for $r_2=10$ cm and $T_0=300$ K maximal transparent carcass temperature is lower than that of opaque carcass at any fuel flow rates and at $T_0=1100$ K this relation changes at large flow rates, Fig.2 c). For RB of larger radius maximal transparent carcass temperature exceeds that of opaque one when increasing mass fuel flow rate, Fig. 2 a), b).

As follows from Fig.3, at low fuel flow rates combustion front in transparent carcass localizes longer from the center than in opaque one. This is related to higher radiation heat losses from hot area. When increasing flow rate, this situation either remains unchanged or becomes opposite. Obviously, this is related to the fact that a strong radiation flow directed towards gas occurs, resulting in heat recuperation in the system. Therefore, inversion of maximal transparent and opaque carcass temperatures, Fig.2, corresponds to those system parameters at which combustion in transparent carcass is localized greatly closer to the center than in opaque one, Fig.3.

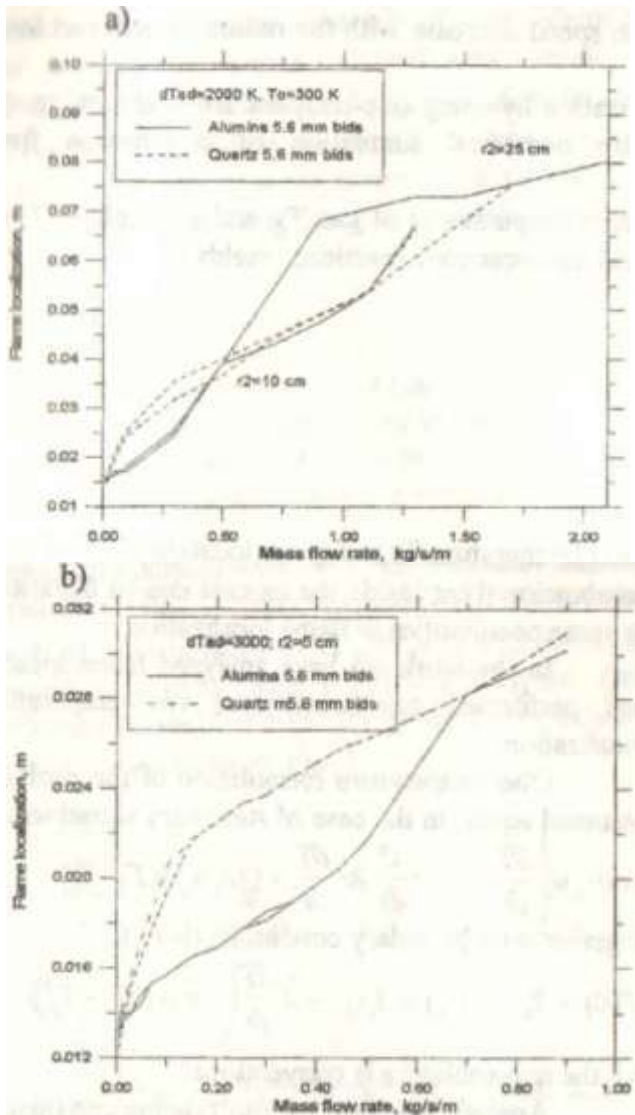


Fig. 3. Combustion localization radius for RB of transparent (quartz) and opaque (Al_2O_3) beds, depending on mass fuel flow rate, a) - $dT_{ad}=2000\text{ K}$, b) - 3000 K .

Certain unmonotonous nature of combustion localization curves (availability of bends) given in Fig.3 is related to influence heat discharge at internal and external carcass radii (boundary conditions) as well as to radial change of temperature, gas filtration rate and interphase heat transfer intensity.

Conclusion

Using transparent beds with quantum path length exceeding pore size several times enables one to increase radiation efficiency of RB by 2-5% at system parameters and ambient temperature considered in the article, Fig.1 At higher ambient temperatures typical for heat-treatment furnaces, gain in efficiency by using transparent beds decreases at low flow rates and fuel heat content. Therefore, applying transparent beds for RB that are used in heat-treatment furnaces needs feasibility study, regarding thermo-physical system peculiarities mentioned in the article.

Using transparent beds allows to reduce maximal temperature of the carcass by 50 - 150 K for the conditions simulated in the work However, this reduction may disappear or even opposite results is possible for systems with larger radius ($r_2>10\text{ cm}$ for the system

parameters considered in the work) Fig.2, due to increase of recuperation effectiveness inside porous carcass. Effect of higher heat recuperation intensity at filtration combustion in transparent porous bodies can be used to improve adiabatic combustion regimes.